Physica A 460 (2016) 1–15

Contents lists available at ScienceDirect

Physica A

journal homepage: www.elsevier.com/locate/physa

Unstable network fragmentation in co-evolution of Potts spins and system topology

Joanna Toruniewska [a], Krzysztof Suchecki [a], Janusz A. Hołyst [a,b,*]

[a] Center of Excellence for Complex Systems Research, Faculty of Physics, Warsaw University of Technology, Koszykowa 75, PL-00662 Warsaw, Poland

[b] ITMO University, 19 Kronverkskiy av., 197101 Saint Petersburg, Russia

HIGHLIGHTS

- A fragmented network is unstable in quasi-ergodic coevolution.
- The system slowly evolves towards a single fully ordered component.
- Dynamics of clusters "surfaces" is responsible for the transition shape.

ARTICLE INFO

Article history:
Received 21 August 2015
Received in revised form 22 December 2015
Available online 27 April 2016

Keywords:
Complex networks
Coevolution
Potts model
Fragmentation

ABSTRACT

We investigate co-evolution of discrete q-state Potts model and the underlying network topology, where spin changes and link re-wiring follow the same canonical ensemble dynamics in a constant temperature. It means that there are no absorbing, frozen states present in our model. Depending on the temperature T and probability of link dynamics p the system can exist in one of three states: ordered, disordered and ordered clusters (fragmented network), with the last being unstable and slowly relaxing into ordered state. The transition from ordered clusters to globally ordered system is characterized by non-exponential, slow growth of the order parameter. We investigate this process analytically and explain the transition characteristics as the result of the dominance of activity of "surface" nodes in each ordered cluster, as opposed to "bulk" nodes that are inactive.

1. Introduction

Many different systems that are subject of research in natural and social sciences can be described as networks [1]. Processes found in such systems can be often described in terms of dynamics on the network, where internal variables of the nodes change, or dynamics of the network, where connections are changing. While most dynamical processes involving networks can be classified as either of those two, an interesting topic of research is the interaction between them, often called co-evolution or adaptive networks [2,3]. Special attention has been given to co-evolution of models displaying emergence of cooperation or same-state domains, such as voter model [4,5], Ising-like model [6], models based on game theory [3] and also oscillator synchronization [7]. An interesting process observed is the *fragmentation transition*, where the system

* Corresponding author at: Center of Excellence for Complex Systems Research, Faculty of Physics, Warsaw University of Technology, Koszykowa 75, PL-00662 Warsaw, Poland.
E-mail address: jholyst@if.pw.edu.pl (J.A. Hołyst).

http://dx.doi.org/10.1016/j.physa.2016.04.029
0378-4371/

splits into topologically separate domains or clusters, each displaying internal order. A common feature found in most of these models is the fact that they have an *absorbing state* and the fragmented network is one of such states. The process depends not only on model parameters, but also on an initial system state [8], since existence of absorbing states means non-ergodicity.

In this work, we investigate the co-evolution of discrete q-state Potts model and rewiring of connection. The Potts model, as a generalization of Ising model, has been widely studied [9]. Of special interest are phase transitions, that have been investigated in various topologies, starting from periodic lattices [9], Bethe lattice [10], Apollonian networks [11] and complex networks [12–14]. Depending on the number of states q, the discrete Potts model is equivalent to the Ising model (for $q = 2$, we discuss this more thoroughly in Section 2), possesses the same properties as percolation ($q \to 1$) [15] or features discontinuous phase transition along the typical continuous one ($q > 2$) [12,14]. The propensity of the Potts model to generate homogeneous domains in low temperatures allowed its application for detecting community structure of a network [16–18]. The inverse Potts model has been also recently applied to reconstruct a real social network (Italian parliament) [19].

In our work, both Potts model and the connection dynamics follow the canonical ensemble under constant temperature. We show with numerical simulations, that unlike in similar models where non-homogeneous absorbing state is present [6], the state of ordered clusters that occurs due to fragmentation is a transient state in finite systems and that the system relaxes into a single ordered cluster. We investigate and explain evolution of the order parameter during this transition.

Section 2 describes the model and its implementation in simulations, Section 3 discusses phase diagram, Section 4 describes all assumptions used, Section 5 shows the analytical description of the phenomena and Section 6 offers summary and concluding remarks.

2. Model

We analyze discrete Potts model on a complex network, where node states are co-evolving with network connections. We consider a fixed set of N nodes, each node i possessing a Potts spin $s_i \in 1, 2, \ldots, q$ with q being model parameter. The nodes are connected by edges, which can be described by an adjacency matrix A, where $A_{ij} = A_{ji} = 1$ when nodes i and j are connected and $A_{ij} = 0$ when they are not.

We assume same interaction strength J between all interacting pairs of spins, so the Hamiltonian of the system can be written as

$$H = -J \sum_{i,j} A_{ij} \delta_{s_i, s_j}, \tag{1}$$

where δ is the Kronecker delta and $J > 0$ is the coupling constant (we consider only ferromagnetic interactions). Since only a difference in energies possesses a physical meaning, not energy values themselves, for $q = 2$ this Hamiltonian is equivalent to that of the well-known Ising model without an external field. Note that the discrete Potts model is not equivalent to the Ising model with more spin states (for example $s_i \in \{-1, 0, 1\}$). In fact for the Potts model, the only possible energy of interactions corresponds to matching or unmatching neighboring spins, while in the Ising model with higher spins such energy can possess more values. Different states in the Potts model can be treated as "orthogonal",[1] unlike different scalar values corresponding to the Ising model. We allow changes of both node states and links between nodes, although topology dynamics consists only of rewiring, keeping the number of links constant. Both spin and link dynamics follow the same principle as Metropolis algorithm, where changes are proposed and accepted or rejected based with probability $e^{-\beta \Delta H}$. During an update of a node, we either attempt changing the node state (as in the regular Potts model) or changing the other endpoint of incident edge. Edge dynamic is attempted with a fixed probability p, which is a system parameter. The system is treated as being in a constant temperature T, scaled in J/k_B units, meaning that $J = 1$ and $\beta = 1/T$.

In the simulations, we have used an asynchronous update rule, where each time step consists of N single updates of randomly chosen nodes (attempting to change either state or one of incident links). While the update rule can have a significant impact on the model dynamics, the Metropolis algorithm relies on single state changes to efficiently probe phase space. An alternative would be to use a synchronous approach. This would however mean either defeating purpose of Metropolis algorithm and random phase space search or discrepancy between probabilities of state change and energy difference if single transition probabilities are used. Such discrepancy may lead to artificial behaviors, such as oscillatory states in the Ising model [20]. Since our aim was to base system dynamics on the Hamiltonian, we used Metropolis algorithm and kept the asynchronous update as the only considered rule. The co-evolutionary dynamics is frequently considered as applying to social systems. In fact, humans do not act according to one common clock, and interactions between them – exchange of information and opinions, influencing each other – are not synchronized. Therefore in such a situation, the asynchronous updating is very well justified.

[1] If we use product of spins in the Hamiltonian (as in Ising model) $H = -J \sum_{i,j} s_i s_j$ but treat different states $s = 1, 2, 3, \ldots$ as orthogonal unit vectors in q dimensional space then the scalar product is equivalent to the δ_{s_i, s_j}.

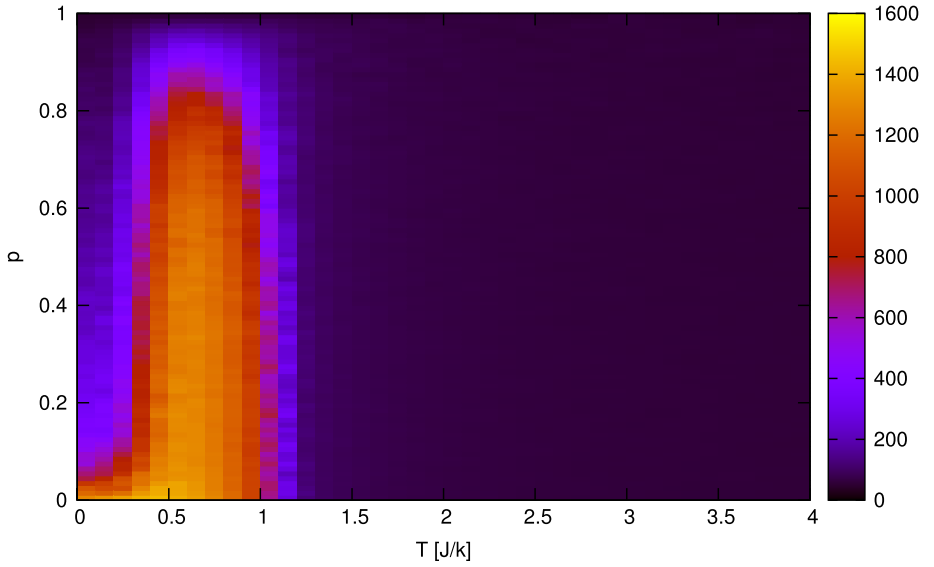

Fig. 1. Order parameter M dependence on temperature T and probability p. Data are obtained from numerical simulation on a graph with $N = 1000$, $\langle k \rangle = 4$ and number of states $q = 5$. Data are averaged over 100 time steps, with prior 100 time steps skipped. There is an ordered cluster phase for $T < 0.3$, an ordered phase for $0.3 < T < 1$ and a disordered phase for $T > 1$.

3. Stability of ordered clusters

We have first explored the parameter space (T, p) numerically and monitored the behavior of the order parameter M (equivalent to magnetization) and the number of interfaces I (number of links connecting nodes with different states). The order parameter of our system is defined as

$$M = \sum_{s=1}^{q} \left| N_s - \frac{N}{q} \right| \tag{2}$$

where N_s is the number of spins with value s. It correctly distinguishes disordered and ordered phases regardless of which of the q states is dominant. We would like to note, that unlike magnetization, for $q > 2$ our order parameter can take values greater than N:

$$M_{max} = \left| N - \frac{N}{q} \right| + \sum_{s \neq s_0} \left| 0 - \frac{N}{q} \right| = N \left(1 + \frac{q-2}{q} \right) \tag{3}$$

which means that M_{max} varies between N for $q = 2$ and $2N$ for $q \to +\infty$. For $q = 2$, it reduces to $|N_1 - N_2|$ which is equivalent to the absolute value of magnetization in the Ising model.

We have used the Erdös–Rényi random graph with $N = 1000$ nodes and mean degree $\langle k \rangle = 4$ as an initial topology of the network, while the number of possible node states was equal to $q = 5$. The initial node states were random with equal probability for any of the q different values.

Based on the results seen in Figs. 1 and 2, we can identify three regions of the parameter space: the ordered phase, the disordered phase and the region of ordered clusters. The schematic structure of the system in these states has been shown in Fig. 3.

For the parameters used in the simulations the ordered phase appears to exist for $0.3 < T < 1$, where most of nodes have the same state (interface number I is low and order parameter M is high). Disordered phase occurs in temperature $T > 1$, where nodes have mostly random states (order parameter M is low and interface number I is high). When $T < 0.3$ we observe network fragmentation — the system assumes the state of ordered clusters, with both the order parameter M and number of interfaces I low. The values of M and I can be explained by approximately similar number of nodes in each of the q states (meaning the global order parameter M is low) and nodes being connected mostly to other nodes in the same ordered domain (meaning the number of interfaces I is also low). The phenomenon of network fragmentation is well known for other co-evolving systems [4,5]. A distinct feature of most co-evolving systems examined so far is the existence of absorbing states, meaning the system is not ergodic. Our model does not feature absorbing states and is quasi-ergodic (as most spin models, including Potts and Ising models, existence of two or more ordered states with different magnetizations means they are not fully ergodic since initial conditions will determine which of these states is reached in equilibrium).

More in-depth investigation shows that the ordered clusters are unstable. If the simulations are run for a long time, the system arrives at a globally ordered state. This means that the ordered clusters are not a true phase, but merely a transient,

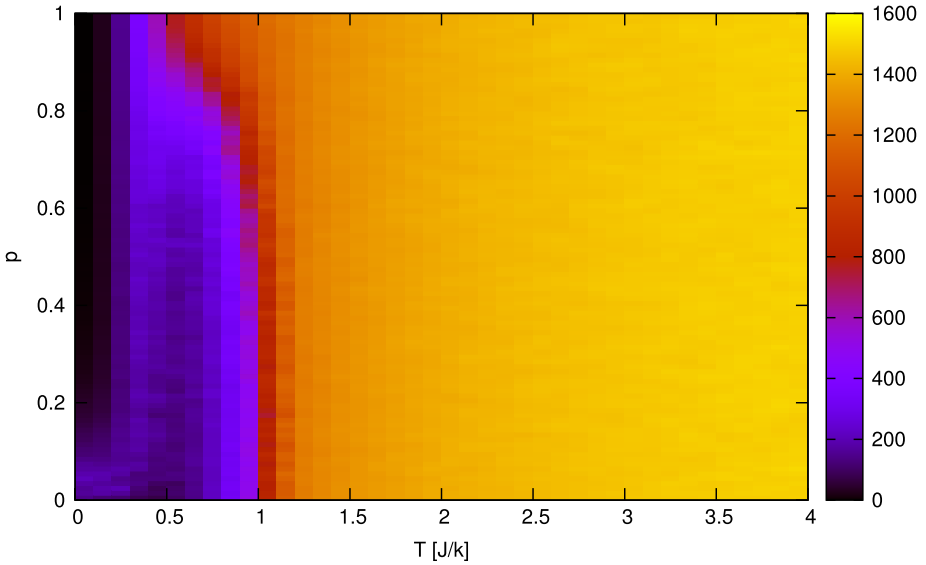

Fig. 2. Number of interfaces I (links between nodes in different state) dependence on temperature T and probability p. Data are obtained from numerical simulation on a graph with $N = 1000$, $\langle k \rangle = 4$ and number of states $q = 5$. Data are averaged over 100 time steps, with prior 100 time steps skipped. There is ordered cluster phase for $T < 0.3$, ordered phase for $0.3 < T < 1$ and disordered phase for $T > 1$.

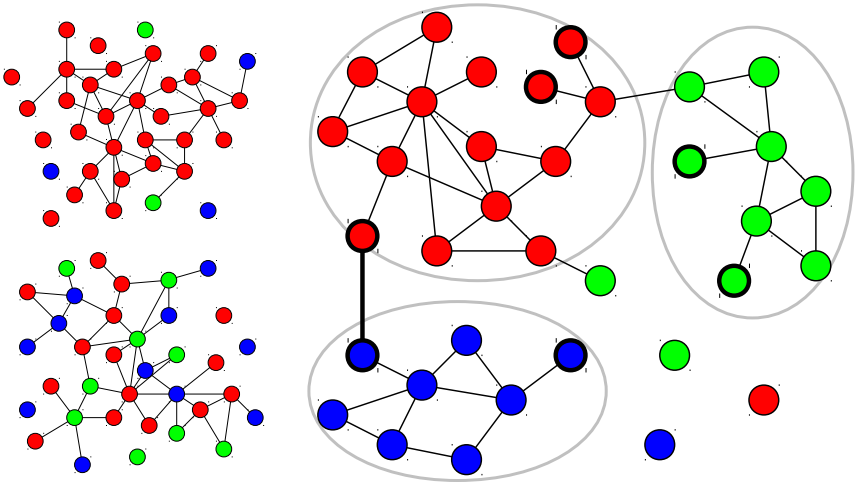

Fig. 3. Schematic structure of the system in the ordered (*top left*), the disordered (*bottom left*) and the ordered clusters (*right*) state. The ordered cluster state consists of ordered clusters (encircled in grey ovals), featuring dominant (red) as well as secondary clusters (green, blue) as well as mismatched nodes attached to clusters (one green attached to red cluster) and disconnected nodes (in lower right part) (visualization of assumption 2). The surface nodes in clusters (having only one link to own cluster) are highlighted with thick borders. Inter-cluster links that connect at least on surface node (marked by thick line here) are responsible for dynamics of cluster sizes (see Section 5). (For interpretation of the references to color in this figure legend, the reader is referred to the web version of this article.)

non-equilibrium state of the system. The order parameter value in long-lasting simulations presented at Fig. 4 show that the order parameter is high through all the low temperatures, including region identified as ordered clusters. Additionally, the simulations starting from full ordering yield the same result as those starting from random state, showing that the final result does not depend on initial conditions (except for which specific state dominates the ordered system).

It is worth to note that the transition from ordered clusters to global order is slow — starting from random initial conditions (for $N = 1000, q = 5, T = 0.2, p = 0.5$) it takes only around 50 timesteps for ordered clusters to form, but it could take as long as 7000 timesteps until the system is fully ordered. Moreover, the transition proceeds in an interesting fashion, with the order parameter increasing roughly linearly in time (Fig. 5). This characteristic is partially obscured when the results are averaged (Fig. 6), as different realizations may be characterized by different slopes, which is related to some differences in system structures (numbers and sizes of ordered clusters of different states).

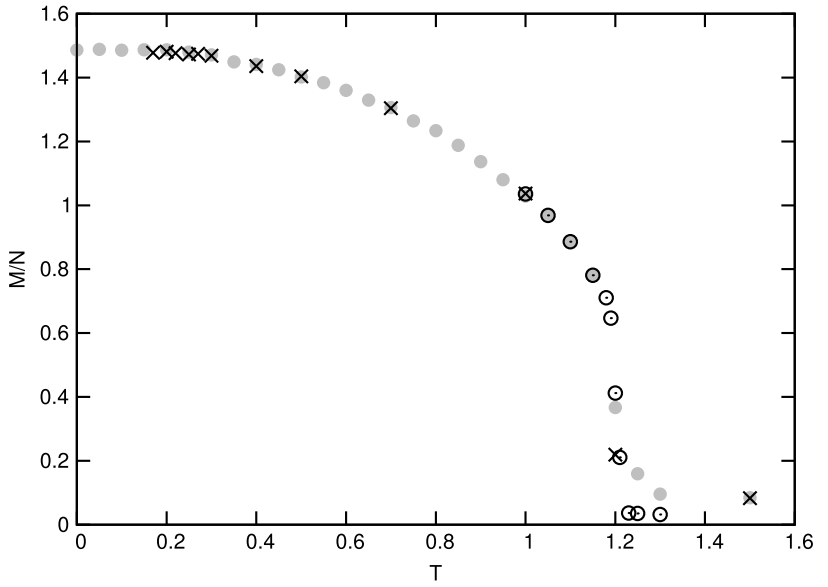

Fig. 4. The order parameter per node M/N in the stable state for different temperatures T. Grey circles represent results for a fully ordered E–R network with $N = 1000$ as initial condition, empty black circles represent results for $N = 10{,}000$, while black X symbols represent results for random initial conditions with $N = 1000$. It is evident that the stable state does not depend on initial conditions, showing that ordered clusters (seen for $T < 0.3$ for used parameters) are just transient state at low temperatures. The data is averaged over 10 simulations for $\langle k \rangle = 4$, $q = 5$ and $p = 0.5$.

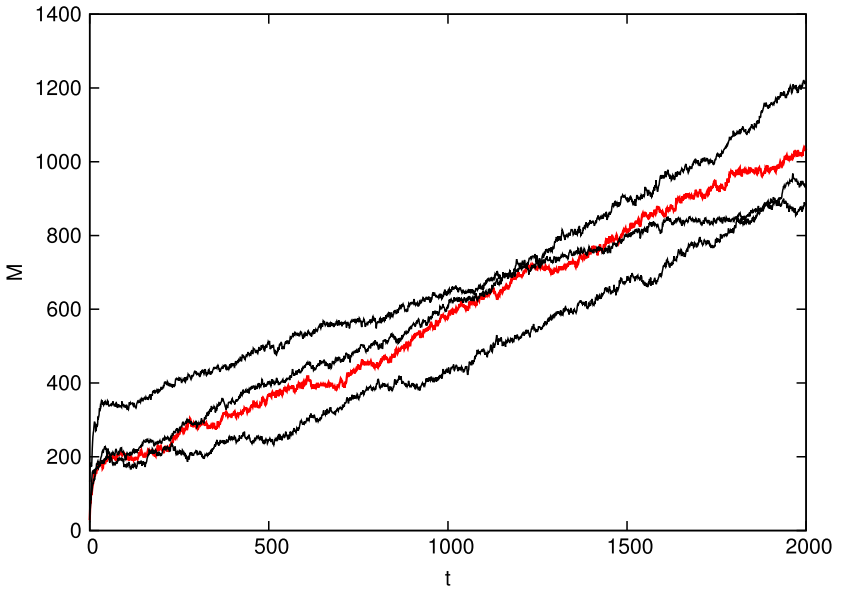

Fig. 5. Time evolution of the order parameter M for several realizations, showing roughly linear increase in value in time. The red line shows the realization later used in Fig. 15. Data obtained for random initial conditions, with $N = 1000$, $\langle k \rangle = 4$, $q = 5$ and $p = 0.5$.

We have used the averaged order parameter and fitted straight lines to parts of the data to obtain an indication of the speeds at which the transition takes place (slope of $M(t)$). This speed strongly depends on the temperature, as shown in Fig. 8 and also depends on the system size (Fig. 7).

To investigate the relaxation of ordered clusters in-depth, we have made several assumptions simplifying the problem, as outlined in the following section.

4. Assumptions

In order to describe analytically the complicated dynamics of the ordered clusters state, we have made a number of assumptions and approximations regarding its structure and the dynamics. We also limit ourselves to using a set of

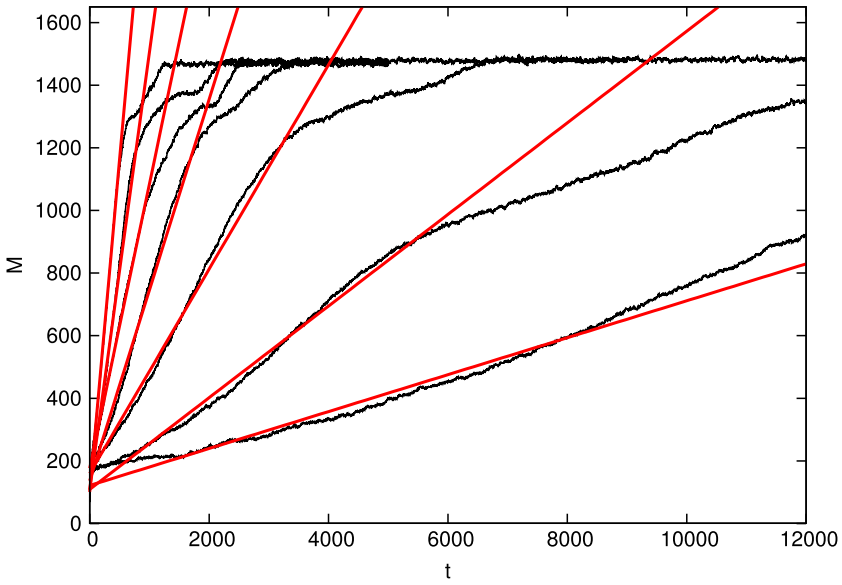

Fig. 6. The order parameter M dependence on time t for different temperatures (in order of decreasing slope 0.25, 0.22, 0.2, 0.17, 0.15). While the growth is nonlinear, lines fitted to the roughly linear part allow rough measurement of the speed of the process. Data are obtained from 10 realizations of numerical simulations with $N = 1000$, $\langle k \rangle = 4$, $q = 5$, $p = 0.5$ with random initial conditions.

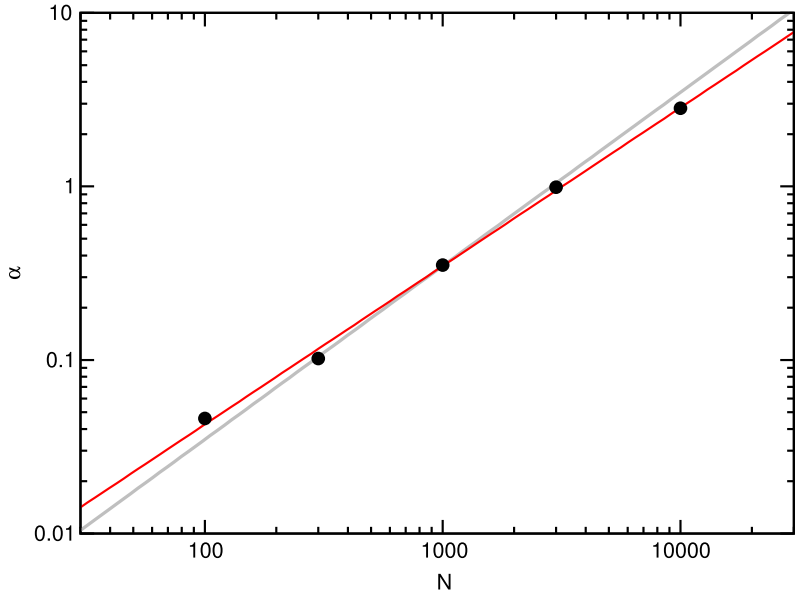

Fig. 7. The transition speed α (slope of the $M(t)$) as a function of the system size N. The dependence is quite close to linear (constant per-node value). The points represent numerical results, the red line represents a linear fit with slope $a = 0.91 \pm 0.02$, while the grey line represents slope 1. Data are obtained from numerical simulation with $\langle k \rangle = 4$, $q = 5$, $T = 0.2$, $p = 0.5$ and averaged over 10 realization with random initial conditions. (For interpretation of the references to color in this figure legend, the reader is referred to the web version of this article.)

parameters $N = 1000$, $q = 5$, $p = 0.5$, $T = 0.2$, $\langle k \rangle = 4$ and $N_A(0) = 320$ (see assumption 8) except cases where other values are explicitly investigated. Below we list all our assumptions, with 1 and 2 forming the basis of our description, while the next assumptions are used for analytical calculations further on.

1. We model our ordered clusters phase as consisting of several distinct clusters. A cluster is defined as a contiguous group of nodes having the same state. Connections between nodes of different states are always inter-cluster connections.
2. The system contains N nodes and consists of (a) a single dominant cluster A of size N_A characterized by the node state s_A; (b) $q - 1$ secondary clusters of same size N_B characterized by other node states; (c) N_f single mismatched nodes attached to clusters; (d) N_1 single, unconnected nodes (see Fig. 9). We ignore size differences between non-dominant clusters and the possibility of other small clusters existing in the system. Fig. 3 shows the schematic structure of ordered clusters state.

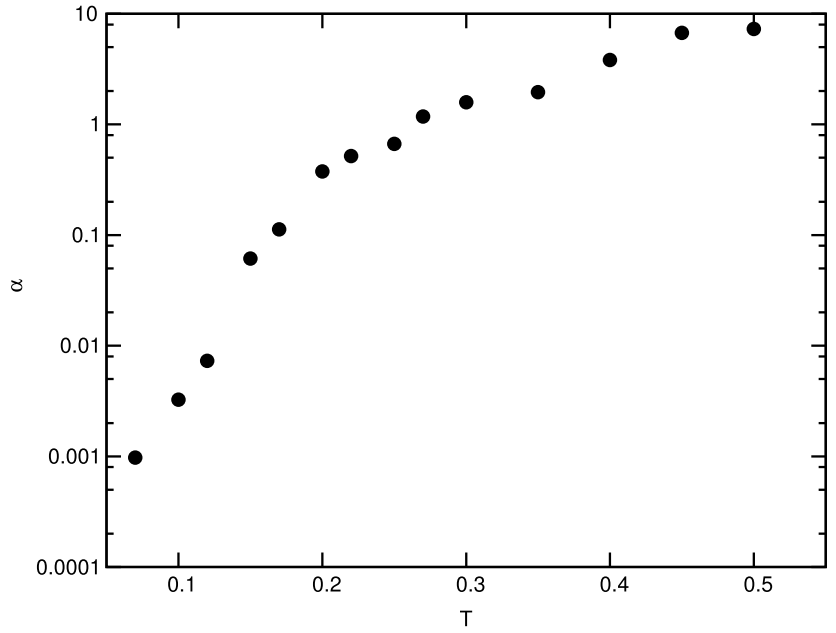

Fig. 8. Dependence of the transition speed α (slope of the $M(t)$) on the temperature T. Data are obtained from numerical simulation on with $N = 1000$, $\langle k \rangle = 4$, $q = 5$, $p = 0.5$ and averaged over 10 realization with random initial conditions.

3. The system is in equilibrium, except for the cluster sizes that change slowly. Our transition is therefore a quasi-static equilibrium process.
4. The equilibrium numbers of unconnected nodes N_1 is constant and depends only on the total system size N and the link density $\langle k \rangle$. Numerical simulations show that the exact value of N_1 plays only a minor role.
5. In low temperatures that we investigate, the connections between clusters are rare, and thus any given node i has either no inter-cluster connections, or only a single one.
6. The inter-cluster connections are distributed evenly across all pairs of nodes belonging to different clusters, just like edges in Erdös–Rényi graph, with ρ being the probability for a pair to be connected (which is low, in accordance with assumption 5).
7. We use a non-linear fit to numerical data to determine the dependence of "surface" (see Section 5) of cluster on their size $S(N_c)$. We also approximate number of unconnected nodes N_1 through numerical simulations. For $N = 1000$ and $q = 5$, the fitting gives

$$S(N_c) = (N_c^a \cdot b + c) \cdot (1 - \mathrm{e}^{-\frac{N_c}{d}}) \tag{4}$$

   where $a = 3.46$, $b = 2.2 \cdot 10^{-9}$, $c = 15.9$, $d = 40$ (see Fig. 12) and $N_1 = 38$. The surface $S(N_c)$ does not depend on temperature, at least in the investigated range between $T = 0.15$ and $T = 0.3$ (lower temperatures were not investigated due to long simulation times, higher do not form observable ordered clusters).
8. We investigate systems starting from initial conditions in agreement with the assumption 2, not random. The system consists of q separate clusters, with the dominant cluster A of given size N_A and the rest of nodes evenly divided into $q - 1$ clusters. Each cluster is fully ordered and has random graph internal topology (meaning that in practice it may be non-contiguous).

5. Dynamics of ordering

We describe the dynamics of the ordered clusters phase in terms of changing cluster sizes (assumptions 1, 2 and 3). We assume constant N_1 and equal sizes of all non-dominant clusters (assumption 2), and additionally that N_f is small and therefore can be approximated as $N_f \approx 0$ in most cases without introducing significant error. This allows us to express the state of the system along the transition between ordered clusters and global order through a single parameter — the size of the dominant cluster N_A. The size of all secondary clusters N_B can be also expressed as $N_B = (N - N_A - N_1)/(q - 1)$. To better understand what kinds of dynamical processes are responsible for the transition, we observe rates of cluster size changes due to three different types of events (see Fig. 10):

1. node state dynamics
2. network connection dynamics involving single unconnected nodes (connecting to and creation of them)
3. other network connection dynamics (mismatched nodes switching connection to matching cluster and reverse)

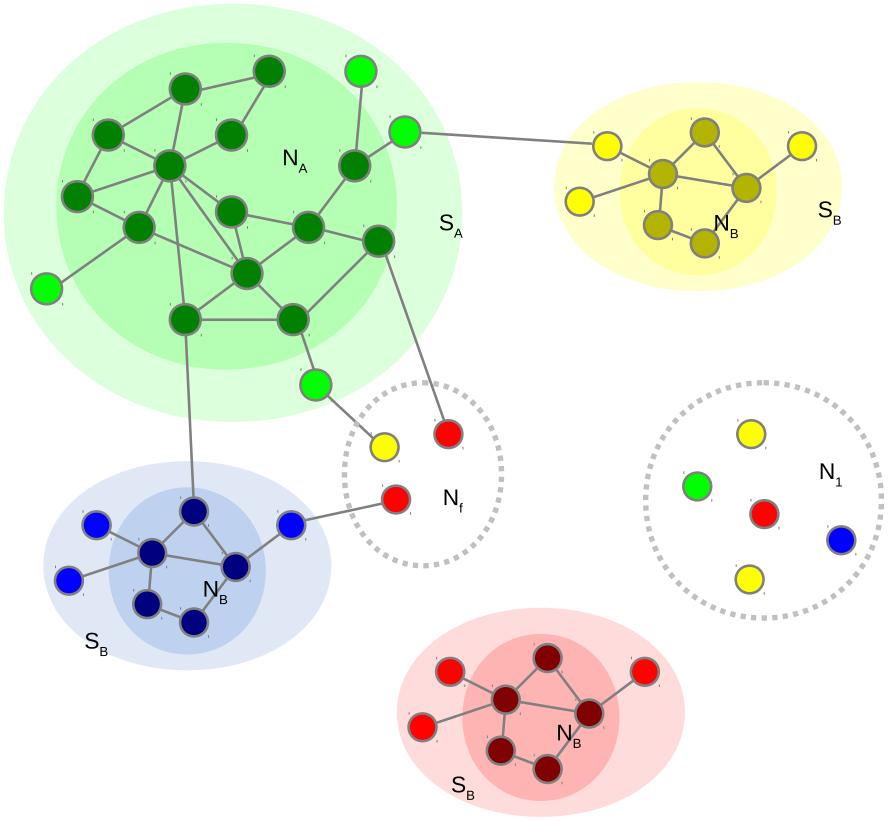

Fig. 9. The structure of the ordered clusters according to the assumptions made (Section 4). The system consists of homogeneous state clusters, with few inter-cluster links. We distinguish a dominant cluster A, $q-1$ secondary clusters B of equal sizes, N_f single mismatched nodes attached to clusters and N_1 single, unconnected nodes. Clusters have S_c surface nodes among the total N_c.

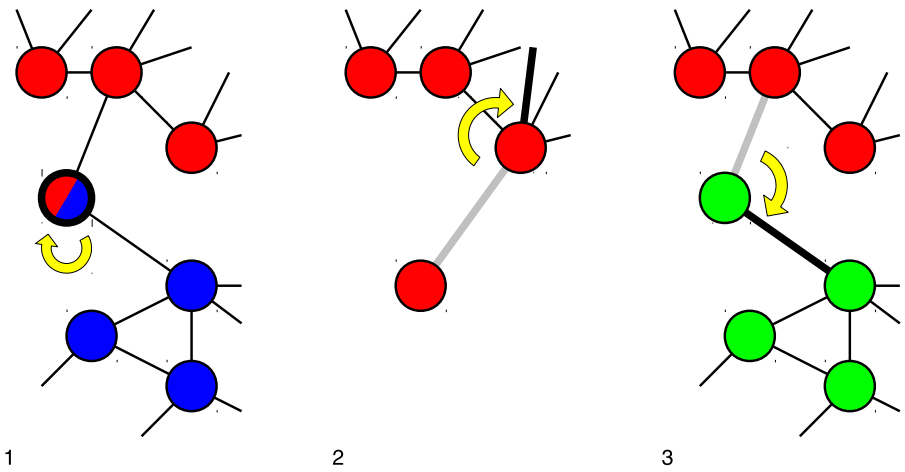

Fig. 10. Three kinds of processes that can change the cluster sizes (from left to right): 1. A node changes its state, leaving its eventual cluster and possibly joining another one; 2. A node in a cluster loses its last connection (grey link) due to rewiring and becomes an unconnected single node; 3. A mismatched node attached to a cluster (grey link) changes its connection to a matching cluster (thick black link). The three categories of processes also include reverse processes to the ones shown in this figure.

Fig. 11 presents dominant cluster size change rates due to three mentioned types of events depending on the size of the cluster.

It is evident that changes caused by network connection dynamics are balanced (in equilibrium, according to assumption 3), but changes due to state dynamics are not, and in fact they show a consistent increase of the dominant cluster size. This

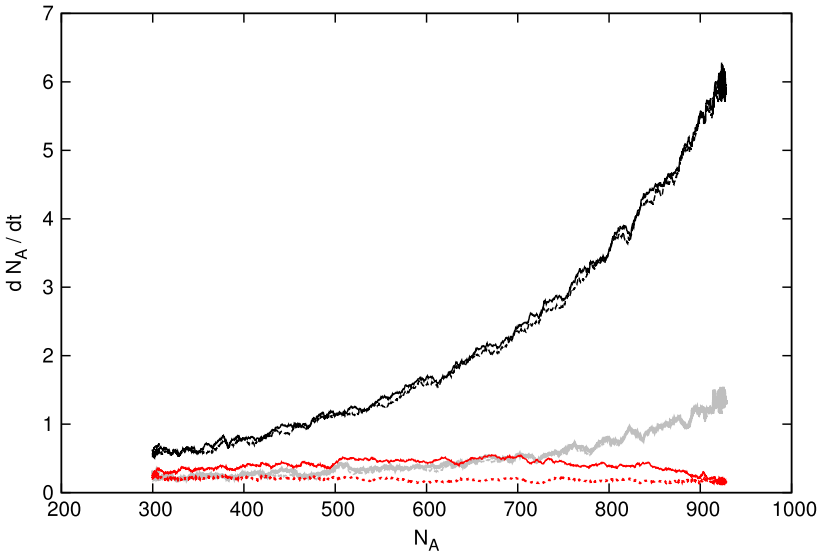

Fig. 11. The dominant cluster size change rates dN_A/dt caused by three types of processes, depending on size of the cluster N_A at the moment. Red lines show changes due to node state dynamics, black lines due to topology dynamics involving unconnected nodes while grey lines are changes due to topology dynamics involving only nodes with connections. Solid lines show positive changes, while dashed lines show absolute values of negative changes. For both black and grey lines, the dashed and solid lines overlap, meaning that the processes are balanced and do not cause net change in cluster size. Red lines show persistent difference, indicating that it is the node state dynamics that is directly responsible for growth of dominant cluster and thus the changes of the order parameter. Data are obtained from numerical simulations with $N = 1000$, $\langle k \rangle = 4$, $q = 5$, $p = 0.5$ and averaged over 20 realizations with a special initial state (assumption 8 with $N_A = 320$). (For interpretation of the references to color in this figure legend, the reader is referred to the web version of this article.)

explains the slow, steady growth of the dominant cluster that causes steady growth of order parameter and leads to the global ordering, when the dominant cluster size reaches the whole system.

The node state dynamics can cause nodes to leave cluster in two different ways: when the node becomes part of another cluster, and when the node becomes mismatched, still attached to the same cluster. We will forget about the second process for now and focus on switching of nodes between clusters. The switch happens when a node i, belonging to a cluster A characterized by the node state s_A and connected to it with $k_{iA} > 0$ links changes its state to match a different cluster B, characterized by the state s_B, to where the node has $k_{iB} > 0$ links. For the node to move to another cluster through node state dynamics, the link to another cluster must be already present, hence $k_{iB} > 0$, but due to rare connections between clusters (assumption 5) it will be only single one, meaning $k_{iB} = 1$. If an update of s_i from s_A to s_B is proposed, the probability to accept such update will be

$$P_i(s_A \to s_B) = \mathrm{e}^{\beta(k_{iB} - k_{iA})} \tag{5}$$

which means that for low temperatures, where the investigated fragmentation occurs, the probability is very low except when $k_{iB} \geq k_{iA}$, meaning $k_{iA} = k_{iB} = 1$. This observation is confirmed by observations of in-cluster degrees of nodes moving between clusters in numerical simulations. Since the energy difference of such a change is zero, its probability does not depend explicitly on the value of temperature and will only depend on the probability of update happening to a node in this specific situation. This depends on the number of nodes connected only with a single link to its own cluster.

We define the *surface* of a cluster as nodes connected to it only by single connections. Because of the reasoning shown above, the surface nodes additionally possessing inter-cluster links are actively switching the clusters they belong to, while the bulk nodes (with in-cluster degrees above 1) have effectively frozen states. The surface of the cluster can change through edge dynamics, as the energy changes during edge rewiring are always 0 or ± 1, regardless of the involved node degrees. This makes it possible for bulk nodes to become surface nodes and vice versa, which results in some equilibrium (assumption 3) amount of surface nodes in each cluster.

We have not managed to find analytical relation between cluster size N_c and its surface S_c, but decided to use a non-linear fit to the numerical data and use the obtained dependence $S(N_c)$ (assumption 7). If the following analysis could explain the dynamics, we can therefore conclude that the surface and its size dependence are driving the process.

Based on the above considerations, we can write the equation for the rate of nodes leaving the dominating cluster A as

$$N_{out} = S(N_A)\rho(N - N_A - N_1)\,\frac{1}{q}(1 - p) \tag{6}$$

where $S(N_A)$ is the surface of cluster A (dependent on the total cluster size N_A, see assumption 3) and ρ is the probability of connection between nodes belonging to different clusters (assumption 6) which we calculate later on. This rate is a product of the following factors:

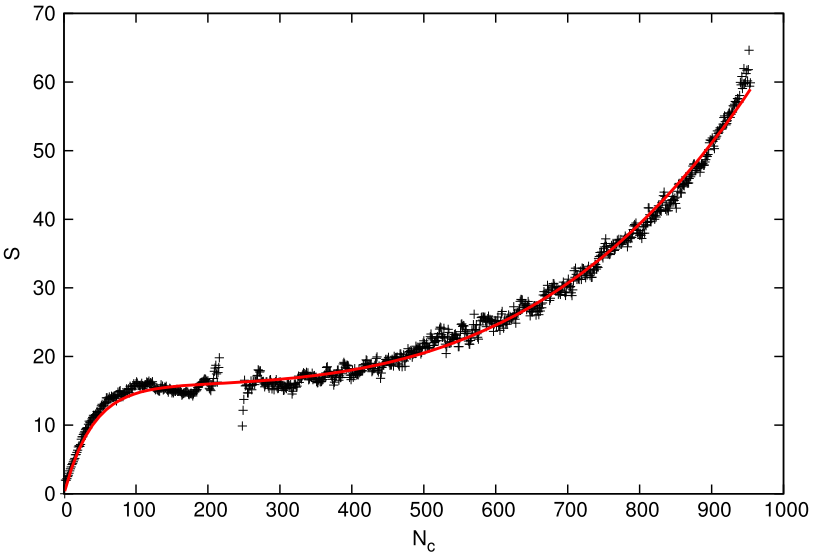

Fig. 12. The dependence of the cluster surface on its total size with fitted curve (Eq. (4)). Data are obtained from numerical simulation on a graph with $N = 1000$, $\langle k \rangle = 4$, $q = 5$, $T = 0.2$ and averaged over 15 realizations. The data for different temperatures are very similar, with differences approximately the same as different realizations. The gap between $N \approx 210$ and $N \approx 250$ comes from the initial conditions where the dominant cluster is set to size $N \approx 250$ which later grows, while secondary clusters start with $N \approx 210$ nodes and shrink afterwards.

1. Mean number of surface nodes updated in single update ($S(N_A)/N$)
2. Number of updates per time step (N)
3. Probability that the updated node has a connection to a different cluster ($\rho(N - N_A - N_1)$) (this is not exact, but because ρ is very small, it is very close)
4. Probability to attempt to change to state that exactly matches the state of the other cluster the node is connected to ($1/q$)
5. Probability of attempting the node state dynamics ($1 - p$)
6. Probability of accepting the change (1, since energy difference is always zero under the circumstances).

Similarly, we can write an equation for the rate of nodes entering the dominant cluster as a sum of rates of nodes leaving all other $q - 1$ clusters and joining cluster A

$$N_{in} = \sum_{c \neq A} S_c \, \rho \, N_A \, \frac{1}{q}(1 - p) = \frac{q - 1}{q} \, S(N_B) \, \rho \, N_A (1 - p) \tag{7}$$

where S_c is the surface of each large cluster, and the sum is over all non-dominant clusters. Based on assumption 2, each non-dominant cluster has the same size N_B and therefore the same surface $S(N_B)$, allowing us to write $\sum_c S_c = (q - 1)S(N_B)$. The connection density ρ is related with the number of interfaces I, as any connection between different clusters is an interface and any interface is a link between different clusters or between cluster and mismatched node. In accordance with assumption 6, the total number of edges between different clusters can be written as

$$I = \rho N_A (N - N_A - N_1) + \rho \frac{(q - 1)(q - 2)}{2} \frac{(N - N_A - N_1)^2}{(q - 1)^2} + \rho N_f (N - N_1). \tag{8}$$

The last component $N_f(N - N_1)$ is a rough approximation of the number of potential interfaces between mismatched nodes and clusters (it neglects the fact that one of the clusters is in matching state as well as the fact that nodes in N_f are known beforehand to have one interface). This value is negligible until the system is close to order and $N - N_A - N_1$ approaches zero, where it becomes leading term, but at the same time it becomes more accurate. To avoid lengthy distractions from the main thought line, calculation of $N_f = N_f(N_A)$ has been shown in the Appendix.

Since we assume that the system is quasi-static (assumption 3), we can say that the number of interfaces is a result of an equilibrium between creation and removal of interfaces. The creation is a result of a node rewiring one of its in-cluster connections to another cluster, while removal is the reverse. The probability that a new interface is created in a single update, which is equal to interface creation rate, is

$$\begin{aligned} I_+ = {} & p \left(1 - \frac{2I}{N}\right) \mathrm{e}^{-\beta} \left[\frac{N_A}{N} \frac{N - N_A - \frac{N_1}{q}}{N} + (q - 1) \frac{N_B}{N} \frac{N - N_B - \frac{N_1}{q}}{N} \right] \\ & + (1 - p) \mathrm{e}^{-\beta} \frac{S(N_A) + (q - 1)S(N_B)}{N} \frac{q - 1}{q} \end{aligned} \tag{9}$$

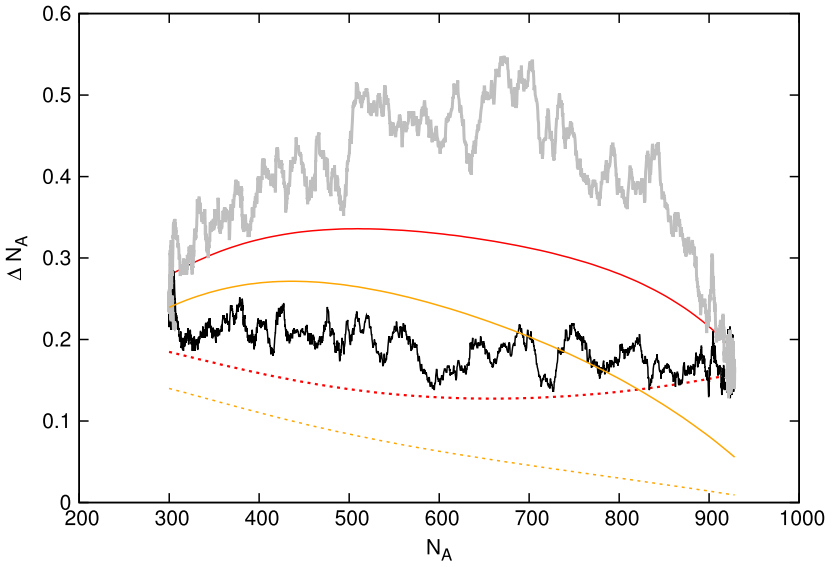

Fig. 13. The rates N_{in}, N_{out} of nodes leaving and entering dominant cluster due to node state dynamics. Black and grey lines show numbers of nodes joining and leaving dominant cluster, measured in numerical simulations (these are same as red lines on Fig. 11). Orange lines show the analytical predictions (solid for joining — Eq. (7), dashed for leaving — Eq. (6)). Red lines show analytical predictions that take node state fluctuations into account (Eqs. (12), (11)) with solid line for joining and dashed for leaving nodes. (For interpretation of the references to color in this figure legend, the reader is referred to the web version of this article.)

while the respective rate of interface removal is

$$I_- = p\frac{2I}{N\langle k\rangle}\left[\frac{N_A}{N}\frac{N_A+\frac{N_1}{q}}{N}+(q-1)\frac{N_B}{N}\frac{N_B+\frac{N_1}{q}}{N}\right]+(1-p)\frac{N_f}{N}\frac{1}{q}. \tag{10}$$

In both equations, the last term proportional to $1-p$ is an effect of node state changes, which produce (in the first equation) or remove (in the second) mismatched nodes attached to clusters.

Knowing that $N_B = (N - N_A - N_1)/(q-1)$ and using both rates, it is easy to obtain an expression for the equilibrium ($I_+ = I_-$) number of interfaces I, dependent on the size of the dominant cluster N_A (not shown, due to expression length). Comparing the equilibrium number of interfaces I and Eq. (8), we can determine the value of ρ in the system.

Using the obtained value of ρ as well as surface size values obtained from fit to numerical data (Eq. (4)), we have calculated expected rates of nodes leaving N_{out} and nodes entering N_{in} the dominant cluster due to node state dynamics. The calculated rates are presented at Fig. 13.

While there is a significant discrepancy between our approach and the data from simulations, the basic shapes of the flows are roughly similar. The rate of nodes joining the dominant cluster is always higher than leaving, with the difference remaining the same order of magnitude through the process, and similar to the magnitude observed in simulations. The discrepancy between real rates and analytical predictions can be lessened by taking into account random fluctuations of the node states, previously disregarded due to low value of $e^{-\beta k}$. Since $e^{-\beta k} \ll 1$, the surface nodes with only single matching neighbor dominate the process while "bulk" nodes remain frozen, and therefore only state fluctuations of surface nodes are considered. The rate of nodes leaving dominant cluster through this process can be written as

$$f_-(N_A) = (1-p)\,S_A\,\frac{(q-1)}{q}\,e^{-\beta}. \tag{11}$$

Single mismatched nodes attached to the dominant cluster emerge from the fluctuations, but also from other processes, such as attaching separated nodes or switching surface nodes between clusters through link rewiring. Such nodes merge with the cluster, producing flow of nodes into the dominant cluster

$$f_+(N_A) = N_f\frac{N_A}{N-N_1}(1-p)\frac{1}{q} \tag{12}$$

where $N_f N_A/(N - N_1)$ is the number of mismatched nodes attached to the dominant cluster (see Appendix). Adding the effects of these fluctuations, we obtain corrected $N_{out}(N_A)$ and $N_{in}(N_A)$, presented in Fig. 13 by red lines. Taking state fluctuations into account corrects the discrepancy between analytical predictions and numerical rates $N_{out}(N_A)$, $N_{in}(N_A)$ for N_A approaching $N - N_1$ (when the system becomes globally ordered).

If we use analytical rates $N_{out}(N_A)$ and $N_{in}(N_A)$ (Eqs. (6), (7)) and calculate the changes of the order parameter in time according to our assumptions and approximations, we obtain a growth curve shown in Fig. 14. The curve is qualitatively similar to real one, although there is a significant quantitative disagreement, most importantly in timescale, but also in the

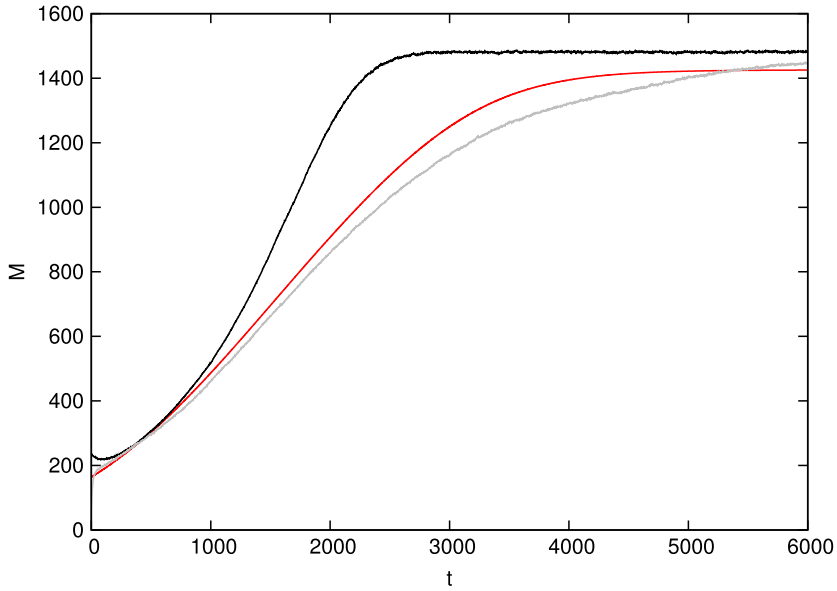

Fig. 14. The dependence of order parameter M on time t. Results of numerical simulations starting from ordered clusters are presented by the black line, analytical results are presented by the red line, while the grey line shows numerical results for random initial conditions. The discrepancy between the analytical and the numerical results is significant, but the shapes of the curves are similar. (For interpretation of the references to color in this figure legend, the reader is referred to the web version of this article.)

final equilibrium value of M. The sources of the discrepancy are our simplified assumptions, reliance on experimental $S(N_A)$ as well as omission of some processes in the quasi-analytical approach.

Our approach explains the observed slow growth of the order parameter through the state changes of node at the cluster "surfaces". An earlier, alternative hypothesis assumed a binomial distribution of node degrees in clusters and thus the node flow rates proportional to the total cluster size. It resulted in predicted lack of any cluster size changes in time. This indicates that the origin of this linear growth is most probably the fact that the surface nodes dynamics dominate, and that the cluster surface is not proportional to the cluster size.

Looking at Figs. 6 and 14, one can notice that the order parameter in the second figure has different shape than in the first. One reason for this discrepancy is the initial conditions, which for Fig. 6 were random, while for 14 were separate ordered clusters, with one dominant in size. For random initial conditions, the sizes of clusters of different states can vary, and some disappear completely before others (Fig. 15), which happens much more rarely when initial conditions mirror our assumptions regarding the network structure.

6. Conclusions

We have investigated the co-evolution of Potts spins and topology of interactions between them in the absence of absorbing states. We found that in a quasi-ergodic system the fragmentation occurs in low temperatures, but the resulting ordered clusters phase is unstable. The system is slowly changing from ordered clusters to global order with the order parameter growing in roughly linear fashion. This slow transition takes place due to steady growth of the largest ordered cluster and is driven by the spin changes of "surface" nodes, i.e. nodes with only single connections to their own clusters. Our semi-analytical approach qualitatively explains the observed behavior of the order parameter in time and identifies microscopic processes responsible for it.

Acknowledgments

The research leading to these results has received funding from the European Union Seventh Framework Programme (FP7/2007–2013) under Grant Agreement No. 317534 (the Sophocles project) and from the Polish Ministry of Science and Higher Education Grant No. 2746/7.PR/2013/2. J.A.H. has been also partially supported by Russian Scientific Foundation, proposal #14-21-00137 and by European Union COST TD1210 *KNOWeSCAPE* action.

Appendix. Calculation of N_f

The number of mismatched nodes N_f attached to a cluster can be estimated using the assumption 3, that states that the process is quasi-static and thus the system is in equilibrium. It is an effect of the balance between creation and removal of mismatched nodes.

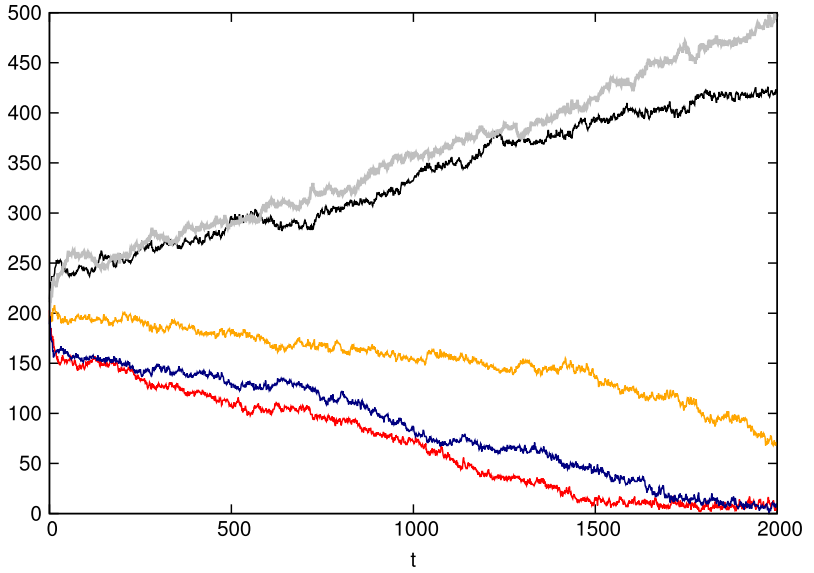

Fig. 15. The number of nodes in every state N_s depending on time t. Data are obtained from numerical simulation on a graph with $N = 1000$, $\langle k \rangle = 4$ and $q = 5$. Initial state of graph was random E–R topology and random node states.

The appendix follows the notation and definitions contained in Section 4. The probabilities of various processes responsible for creation and removal of mismatched nodes (P_{+sAA}, P_{+sBB}, P_{+l1A}, P_{+l1B}, P_{+lBA}, P_{+lBB}, P_{+lAB}, P_{-lx1}, P_{-sxx}, P_{-lAB}, P_{-lBB}, P_{-lBA}) are introduced and calculated later on. We would also like to remind that A signifies dominant cluster (there is only one), while B signifies any of the $q-1$ secondary clusters present in the system.

The processes of creation and removal of mismatched nodes can be split up into several sub-processes each and can be quantitatively expressed as probabilities to occur during a single update. The creation is an aggregation of thermal fluctuations converting surface nodes to mismatched ones (P_{+sAA}, P_{+sBB}), rewiring links inside a cluster so that a previously single, unconnected node with non-matching state is attached to the cluster (P_{+l1A}, P_{+l1B}) and rewiring links that lead to moving of node from one cluster to another (P_{+lBA}, P_{+lBB}, P_{+lAB}). The removal of mismatched nodes is an aggregation of node state changes converting them into members of the clusters (P_{-sxx}), link changes separating them to create single unconnected nodes (P_{-lx1}) as well as attaching them to other clusters (P_{-lAB}, P_{-lBB}, P_{-lBA}). The index of the probability identifies whether it is the probability to create (+) or remove (−) mismatched node and whether it describes the state (s) or link (l) dynamics. Also included is the cluster type the node was attached before and afterwards (A, B, considering topology only, not states) or if they were/are single nodes (1). If the probability encompasses both cluster types then x is substituted instead of A and B.

The probabilities to create mismatched node attached to dominant (P_{+sAA}) or other (P_{+sBB}) cluster through thermal fluctuations can be expressed as

$$P_{+sAA} = (1-p)\frac{S(N_A)}{N}\frac{q-1}{q}\mathrm{e}^{-\beta} \tag{A.1}$$

$$P_{+sBB} = (1-p)\frac{S(N_B)}{N}(q-1)\frac{q-1}{q}\mathrm{e}^{-\beta} \tag{A.2}$$

with the terms corresponding to the probability to update state of a surface node (times $q-1$ secondary clusters in second equation), the probability to attempt changing into mismatched state and finally the probability to accept such change. Note that Eq. (A.1) shows the number of nodes leaving dominant cluster through thermal fluctuations of states and is identical to Eq. (11) in the main article. The probabilities to attach a single unconnected node to dominant cluster are

$$P_{+l1A} = p\frac{N_A}{N}\frac{N_1}{N}\frac{q-1}{q}\mathrm{e}^{-\beta} \tag{A.3}$$

$$P_{+l1B} = p\frac{N_B}{N}(q-1)\frac{N_1}{N}\frac{q-1}{q}\mathrm{e}^{-\beta} \tag{A.4}$$

with the terms corresponding to the probability for updating links of a node in the cluster (times $q-1$ secondary clusters in second equation), the probability of choosing a single node as a new target, the probability that this node has a different state than the considered cluster and finally the probability to accept such change. The probabilities to move the node from

a cluster to a mismatched set attached to another cluster can be expressed as

$$P_{+lBA} = p\frac{S(N_B)}{N}(q-1)\frac{N_A}{N}\mathrm{e}^{-\beta} \tag{A.5}$$

$$P_{+lBB} = p\frac{S(N_B)}{N}(q-1)\frac{N_B}{N}(q-2)\mathrm{e}^{-\beta} \tag{A.6}$$

$$P_{+lAB} = p\frac{S(N_A)}{N}\frac{N_B}{N}(q-1)\mathrm{e}^{-\beta} \tag{A.7}$$

with the terms corresponding to the probability for updating links of a node on surface of a cluster (including the number of these clusters), the probability of choosing specific type of cluster as target of the rewiring (including their eventual number) and the probability to carry out this change.

The probability to merge a mismatched node back into the connected cluster through state dynamics is

$$P_{-sxx} = (1-p)\frac{N_f}{N}\frac{1}{q} \tag{A.8}$$

with the terms corresponding to the probability to update a mismatched node and the probability to change to a state matching the connected cluster. The probability to turn mismatched node into a single, unconnected node is

$$P_{-lx1} = p\frac{N_f}{N}\frac{1}{\langle k\rangle} \tag{A.9}$$

with the terms corresponding to the probability to update the node directly linked to one of mismatched nodes and the probability to update this particular link out of on average $\langle k\rangle$ links it possesses (note that since energy change cannot be positive, it will be always accepted). The probabilities to merge into another cluster through link dynamics can be written as

$$P_{-lAB} = p\frac{\rho_{AB}N_f}{N}\frac{N_B}{N} + p\frac{N_B(q-1)}{N}\frac{\rho_{AB}N_f}{N}\frac{1}{q-1} = 2p\frac{\rho_{AB}N_fN_B}{N^2} \tag{A.10}$$

$$P_{-lBB} = p\frac{\rho_{BB}N_f}{N}\frac{N_B}{N} + p\frac{N_B(q-2)}{N}\frac{\rho_{BB}N_f}{N}\frac{1}{q-2} = 2p\frac{\rho_{BB}N_fN_B}{N^2} \tag{A.11}$$

$$P_{-lBA} = p\frac{\rho_{BA}N_f}{N}\frac{N_A}{N} + p\frac{N_A}{N}\frac{\rho_{BA}N_f}{N} = 2p\frac{\rho_{BA}N_fN_A}{N^2} \tag{A.12}$$

with both sum components corresponding to rewiring the link of the mismatched node and to rewiring link from matching cluster so that the mismatched node becomes part of that cluster (still attached via interface to the original cluster it was attached to). The first components have terms corresponding to the probability of updating link of a mismatched node attached to given cluster type and the probability to rewire to matching cluster. The second components have terms corresponding to the probability of updating links in clusters that can attach the mismatched node, the probability to rewire to a mismatched node, and the probability that this mismatched node actually had the same state. The values of ρ_{AB}, ρ_{BB}, ρ_{BA} are fractions of mismatched nodes being nodes attached to A with state of one of B clusters, attached to any B with state of another B and attached to B with state of A respectively. Assuming that a fraction of mismatched nodes attached to a cluster is proportional to the size of the cluster, we can get the approximate fractions as $\rho_{AB} = \frac{N_A}{N-N_1}$, $\rho_{BB} = \frac{N_B(q-1)}{N-N_1}\frac{q-2}{q-1}$ and $\rho_{BA} = \frac{N_B(q-1)}{N-N_1}\frac{1}{q-1}$.

By adding up all relevant probabilities

$$P_+ = P_{+sAA} + P_{+sBB} + P_{+l1A} + P_{+l1B} + P_{+lBA} + P_{+lBB} + P_{+lAB} \tag{A.13}$$

$$P_- = P_{-sxx} + P_{-lx1} + P_{-lAB} + P_{-lBB} + P_{-lBA} \tag{A.14}$$

we obtain the probabilities to create new mismatched node or remove one in a single update.

Since we assume quasi-stationary process, these probabilities must be balanced $P_+ = P_-$. If we assume that N_f is small, we can write that $N_B \approx (N - N_A - N_1)/(q-1)$ and can express P_+ and P_- solely through N_A, N_f and parameters q, p, N, $\langle k\rangle$. We also notice that P_+ is independent on N_f and P_- can be factorized $P_- = \frac{N_f}{N}P'_-$, where P'_- does not depend on N_f. This means the equilibrium N_f can be easily calculated as

$$N_f = N\frac{P_+}{P'_-} \tag{A.15}$$

and calculated as a function of N_A and the system parameters.

The main article uses N_f value calculated in here in calculation of number of interfaces I (in Eqs. (8) and (10)) as well as rate of mismatched nodes returning to dominant cluster (Eq. (12)).

References

[1] S.N. Dorogovtsev, J.F.F. Mendes, Evolution of Networks: From Biological Nets to the Internet and WWW, Oxford University Press, 2003.
[2] T. Gross, B. Blasius, Adaptive coevolutionary networks: a review, J. R. Soc. Interface 5 (2008) 259–271. http://dx.doi.org/10.1098/rsif.2007.1229.
[3] M. Zimmermann, V. Eguiluz, M. Miguel, Coevolution of dynamical states and interactions in dynamic networks, Phys. Rev. E 69 (6) (2004) 065102. http://dx.doi.org/10.1103/PhysRevE.69.065102.
[4] G. Böhme, T. Gross, Analytical calculation of fragmentation transitions in adaptive networks, Phys. Rev. E 83 (3) (2011) 035101. http://dx.doi.org/10.1103/PhysRevE.83.035101.
[5] F. Vazquez, V. Eguíluz, M. Miguel, Generic absorbing transition in coevolution dynamics, Phys. Rev. Lett. 100 (10) (2008) 108702. http://dx.doi.org/10.1103/PhysRevLett.100.108702.
[6] S. Mandrà, S. Fortunato, C. Castellano, Coevolution of Glauber-like Ising dynamics and topology, Phys. Rev. E 80 (5) (2009) 056105. http://dx.doi.org/10.1103/PhysRevE.80.056105.
[7] M. Li, S. Guan, C.-H. Lai, Formation of modularity in a model of evolving networks, Euro Phys. Lett. 95 (5) (2011) 58004. http://dx.doi.org/10.1209/0295-5075/95/58004.
[8] R. Lambiotte, J. Gonzlez-Avella, On co-evolution and the importance of initial conditions, Physica A 390 (2) (2011) 392–397. http://dx.doi.org/10.1016/j.physa.2010.09.024.
[9] F.Y. Wu, The Potts model, Rev. Modern Phys. 54 (1982) 235–268. http://dx.doi.org/10.1103/RevModPhys.54.235.
[10] N. Ganikhodjaev, F. Mukhamedov, J.F.F. Mendes, On the three state Potts model with competing interactions on the Bethe lattice, J. Stat. Mech. Theory Exp. 2006 (08) (2006) P08012.
[11] N.A.M. Araújo, R.F.S. Andrade, H.J. Herrmann, *q*-state Potts model on the Apollonian network, Phys. Rev. E 82 (2010) 046109. http://dx.doi.org/10.1103/PhysRevE.82.046109.
[12] F. Iglói, L. Turban, First- and second-order phase transitions in scale-free networks, Phys. Rev. E 66 (2002) 036140. http://dx.doi.org/10.1103/PhysRevE.66.036140.
[13] S.N. Dorogovtsev, A.V. Goltsev, J.F.F. Mendes, Potts model on complex networks, Eur. Phys. J. B 38 (2004) 177–182. http://dx.doi.org/10.1140/epjb/e2004-00019-y.
[14] M. Krasnytska, B. Berche, Y. Holovatch, Phase transitions in the Potts model on complex networks, Condens. Matter Phys. 16 (2) (2013) 23602. http://dx.doi.org/10.5488/CMP.16.23602.
[15] C. Fortuin, P. Kasteleyn, On the random-cluster model. I. Introduction and relation to other models, Physica 57 (4) (1972) 536–564. http://dx.doi.org/10.1016/0031-8914(72)90045-6.
[16] J. Reichardt, S. Bornholdt, Detecting fuzzy community structures in complex networks with a Potts model, Phys. Rev. Lett. 93 (21) (2004) 218701. arXiv:cond-mat/0402349, http://dx.doi.org/10.1103/PhysRevLett.93.218701.
[17] H.-J. Li, Y. Wang, L.-Y. Wu, Z.-P. Liu, L. Chen, X.-S. Zhang, Community structure detection based on Potts model and network's spectral characterization, Europhys. Lett. 97 (2012) 48005. http://dx.doi.org/10.1209/0295-5075/97/48005.
[18] R. Lambiotte, M. Ausloos, Uncovering collective listening habits and music genres in bipartite networks, Phys. Rev. E 72 (2005) 066107. http://dx.doi.org/10.1103/PhysRevE.72.066107.
[19] C. Bisconti, A. Corallo, L. Fortunato, A.A. Gentile, A. Massafra, P. Pellè, Reconstruction of a real world social network using the Potts model and loopy belief propagation, Front. Psychol. 6 (1698). http://dx.doi.org/10.3389/fpsyg.2015.01698.
[20] F. Radicchi, D. Vilone, H. Meyer-Ortmanns, Phase transition between synchronous and asynchronous updating algorithms, J. Stat. Phys. 129 (3) (2007) 593–603. http://dx.doi.org/10.1007/s10955-007-9416-8.